*Intra-city variability of PM exposure is driven by carbonaceous sources and correlated with land use variables*

Peishi Gu*, Hugh Z. Li*, Qing Ye*, Ellis S. Robinson*, Joshua S. Apte†, Allen L. Robinson*, Albert A. Presto*,[1]

*Center for Atmospheric Particle Studies, Carnegie Mellon University, Pittsburgh, Pennsylvania, 15213 United States

† Department of Civil, Architectural and Environmental Engineering, University of Texas at Austin, Austin, Texas 78712 United States

1. Corresponding author: apresto@andrew.cmu.edu

**Abstract**

Localized primary emissions of carbonaceous aerosol are the major drivers of intra-city variability of submicron particulate matter ($PM_1$) concentrations. We investigated spatial variations in $PM_1$ composition with mobile sampling in Pittsburgh, Pennsylvania, USA, and performed source apportionment analysis to attribute primary organic aerosol (OA) to traffic (HOA) and cooking OA (COA). In high source impact locations, the $PM_1$ concentration is on average 2 μg $m^{-3}$ (40%) higher than urban background locations. Traffic emissions are the largest source contributing to population-weighted exposures to primary PM. Vehicle-miles travelled (VMT) can be used to reliably predict the concentration of HOA and localized black carbon (BC) in air pollutant spatial models. Restaurant count is a useful but imperfect predictor for COA concentration, likely due to highly variable emissions from individual restaurants. Near-road cooking emissions can be falsely attributed to traffic sources in the absence of PM source apportionment . In Pittsburgh, 28% and 9% of the total population are exposed to >1 μg $m^{-3}$ of traffic- and cooking-related primary emissions, with some populations impacted by both sources. The source mix in many U.S. cities is similar, thus we expect similar PM spatial patterns and increased exposures in high-source areas in other cities.

## 1. Introduction

Ambient fine particulate matter ($PM_{2.5}$) is a complex mixture of components that differ significantly in chemical identities and sources. Long-term exposure to PM is associated with various adverse health effects and increased mortality.[1] PM concentrations vary both between and within cities. Epidemiology and air quality studies have historically focused on inter-city

variability,[2] but the magnitude of intra-city variability is comparable or sometimes greater.[3] There is evidence of association between intra-city PM spatial gradients and adverse health effects within urban areas.[1,4] Such intra-city variations are often caused by localized primary sources of PM emissions.[5] Studies have also shown evidence that emissions from different sources vary in their negative health effects.[6] Thus, it is important to capture the spatial variability of both the concentration and source contributions of PM in urban environments.

In the United States and Europe, the major local emission sources of PM include traffic, cooking, and biomass burning.[7,8] The relationship between traffic and PM spatial variability has been studied extensively.[9,10] Near-road exposures are correlated with respiratory diseases,[4] vascular disease,[11] and negative birth outcomes.[12] Significantly less is known about spatial variations caused by distributed non-traffic sources, such as cooking and biomass burning.

Source contributions to PM can be inferred from geospatial analysis (e.g., the gradient of PM concentration moving away from a roadway) and source-specific chemical fingerprints. For example, urban black carbon (BC) is dominated by diesel vehicle emissions,[13] hopanes[14] are markers of vehicular emissions, and levoglucosan is associated with biomass burning.[15] More recently, source apportionment analysis of Aerosol Mass Spectrometer (AMS) data using positive matrix factorization (PMF)[16] has identified primary and secondary PM components with consistent and comparable source profiles around the world.[17–19]

Mobile sampling with high time resolution instruments is capable of capturing sharp spatial gradients,[20,21] and mobile deployment of sophisticated, chemically-specific instruments like AMS enables PM source apportionment with high spatial resolution. This in turn enables spatially- and source-resolved characterization of PM, which can vastly improve our understanding of human exposures. In this study, we conducted in-motion mobile sampling with an AMS in Allegheny County and Pittsburgh, Pennsylvania, USA (Figure 1). We investigated the PM composition and source impact at 200-meter spatial resolution and explored how this spatial variability (1) is correlated with the geographic covariates that represent local sources and (2) impacts population exposures in different locations. While these data were collected for one city, we expect similar spatial patterns to exist in other cities because the urban source mix is often dominated by traffic and cooking.

## 2. Materials and Methods

The goal of this study is to quantify the spatial variability of PM concentration, composition, and source impact. To achieve this goal, we collected a spatially- and chemically-resolved PM dataset to quantify the contribution from various sources. Spatial patterns of total and source-resolved PM and the correlation between concentration and spatial covariates enable us to identify hotspots associated with specific sources. Further details on the methods are described in the Supplemental Materials.

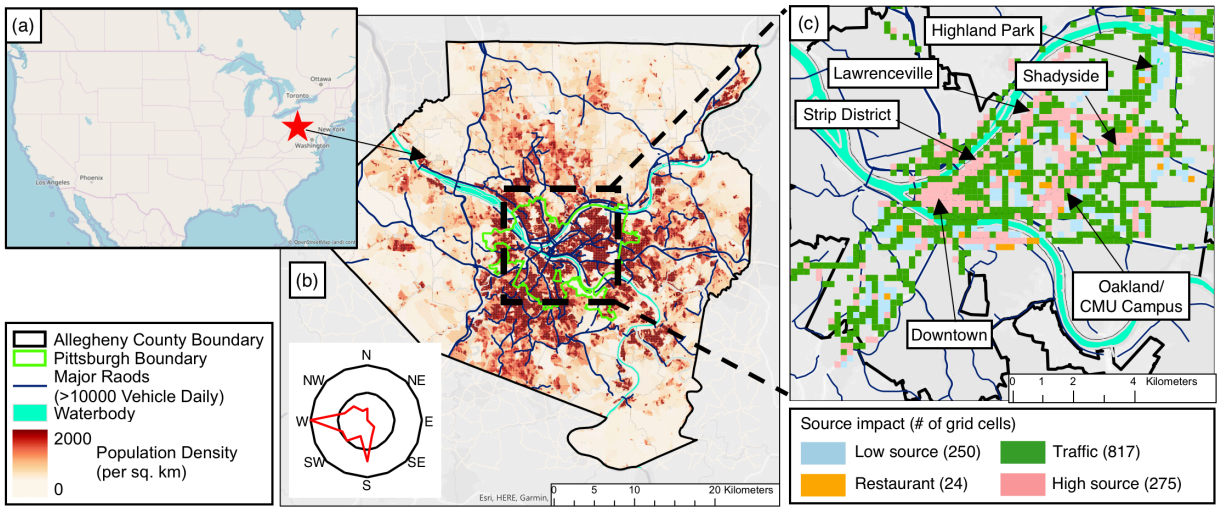


**Figure 1.** (a) Location of Allegheny County and Pittsburgh in the continental US. (b) Boundaries of Allegheny County (black) and the city of Pittsburgh (green), and the residential population distribution. The inset shows the wind frequency distribution. (c) Land-use distribution in sampled areas inside the city of Pittsburgh, gridded at 200m resolution. Several neighborhoods are identified. Details of the sampled neighborhoods are listed Table S1. (Basemap attribution, Sources: Esri, DeLorme, HERE, MapmyIndia)

## 2.1. Mobile sampling platform

Measurements took place in Allegheny County and the city of Pittsburgh, Pennsylvania, USA (Figure 1) as part of the Center for Air, Climate, and Energy Solutions (CACES). We utilized a mobile laboratory[22] with an Aerodyne High-Resolution Aerosol Mass Spectrometer (AMS)[23] and a Magee Scientific Aethalometer (AE-33) onboard. The inlet of the mobile sampling platform is located about 4 meters above ground at the front of the van. We saw no indication of self-sampling during our tests and sampling periods.[24,25] We performed in-motion sampling on 32 different days in summer, fall, and winter from August 2016 to February 2017 (Table S1). The AMS and Aethalometer measurements were made at 20-second resolution, which is equivalent to one sample from every 224 meters at 40 km/h (25 mph). Sixteen communities of roughly 1 $km^2$ area were selected to characterize urban, suburban and rural areas with different land use and source distributions (Table S2). Samples collected on frequently travelled roads between the designated communities were included as well.

Each time we visited a community, we drove through all public roads at least once. Sampling typically took 45-60 minutes per community, and we typically sampled 3-5 communities on each sampling day. For each community, measurements were taken during morning (5-10AM), midday (11AM-4 PM) and evening (5-10 PM) periods on different days, so that concentration data are not biased due to the time-of-day patterns of local emissions. Measurements were only conducted on weekdays to avoid any bias from weekday-weekend emission patterns.

## 2.2. Classification of land-use by traffic and restaurant density

Spatial gradients of PM concentrations exist within a 1-$km^2$ community. Thus, it is necessary to look at the spatial variation at a finer scale relevant to local sources. A 200-by-200-meter grid cell system is used to process spatially-resolved data in this study (the mobile sampling platform collects roughly one sample in every grid cell it passes at 40km/h). All spatial analysis and mapping were performed in Esri ArcGIS Pro (v1.4.1). A total of 1366 cells were visited. The sample size within each 200m grid cell is listed in Figure S1.

We use land-use covariates to classify all the grid cells into four categories (Figure 1c, Table S5) and to quantify the correlation between measurements and local sources. “Low source” cells (250 out of 1366 cells in the sampling domain) have low traffic and no restaurants. Low source cells are mostly in residential areas and parks. “Restaurant” cells (24 out of 1366), which have at least one restaurant and low traffic, are very rare. “Traffic” cells (817 out of 1366), which have

high traffic but zero restaurants, are the most common cells largely due to the on-road sample collection. "High source" cells (275 out of 1366), which have both high traffic and restaurants, are located in business areas such as downtown Pittsburgh. Due to the small number of low traffic restaurant cells, we exclude them from most of the analyses in the manuscript. Details of this classification are described in the SI (Section S.1)

**2.3 Organic PM source apportionment and BC background correction**

Data collected by AMS were processed by Squirrel (v1.57I) and Pika (v1.16I) in Igor (v6.37)[23,26] to determine the concentration of total non-refractive sub-micron PM ($PM_1$), as well as concentrations of various chemical families such as organics, sulfate, nitrate, ammonium, and chloride. We consider the sum of AMS non-refractory $PM_1$ and Aethalometer-measured black carbon (BC) as the total $PM_1$ concentration.

Positive matrix factorization (PMF) analysis was performed on the organic aerosol mass spectra using the AMS PMF tool (1.4.1)[7,27], and yielded a five-factor solution (details in Figure S3, Section S.2). Three primary organic aerosol (POA) factors and two oxidized organic aerosol (OOA) factors were resolved. The three POA factors represent fresh OA emissions from traffic (hydrocarbon-like OA, or "HOA"), cooking (COA) and biomass burning (BBOA). The two OOA factors (more-oxidized organic aerosol, "MOOOA", and less-oxidized organic aerosol, "LOOOA") differ in their molar O:C ratio (0.80 versus 0.52).

Following previous AMS studies, we used the default collection efficiency (CE=0.5) for all species and relative ionization efficiency (RIE=1.4) for organics. Recently published studies have suggested that the default RIE and CE may lead to overestimation of COA concentration, though there seems to be significant variability in RIE for COA.[28,29] We use to the default parameters in this manuscript so that our results remain comparable to other previous field studies.

The BC concentration was determined from the 880-nm channel in the Aethalometer. The BC concentration time series features spikes (Figure S4) associated with local emissions and neighborhood-level enhancements associated with traffic emissions,[24] but a substantial fraction of the BC concentration is not spatially variable. We performed background correction to separate the local, spatially variable BC concentration from the spatially invariant background.

The background correction for BC concentration is demonstrated in Figure S4. First, we smoothed the BC time-series with a second degree polynomial model to remove spikes (Matlab function "smooth" with "span"=30 minutes). These spikes are typically associated with emissions from vehicles or nearby stationary sources.[24] We then fit the baseline of the smoothed curve with

a spline function of the moving 10% quantile (Matlab function "msbackadj" with "WindowSize"=2 hours). We consider the mass concentration below the fitted baseline as the "background" concentration, and the difference between the measured and background concentration as the "local BC" concentration. As shown in Figure S4, the background concentration slowly varies over the course of each sampling day due to changes in the boundary layer height. The local BC contribution captures the individual plumes noted above as well as neighborhood-level enhancements that arise from higher vehicle densities in some areas.

## 3. Results and discussion

### 3.1. Seasonal variation of $PM_1$ concentration, composition, and source contribution

The concentration and composition of $PM_1$ varies greatly by season (Section S.4, Figure S5, SI). In general, $PM_1$ concentration is significantly higher (ANOVA test p-value<0.001) in summer (11.4±5.5 μg $m^{-3}$, average ± standard deviation) than winter (9.1±7.8 μg $m^{-3}$) due to the increased concentrations of secondary oxygenated organic aerosols (less and more oxidized organic aerosols, LOOOA and MOOOA) and sulfate. These are the result of enhanced photochemical oxidation in the hotter season.[30,31] Concentrations of primary components - traffic-related OA (HOA), cooking-related OA (COA) and local BC - show much less seasonal variability. Biomass burning-related OA (BBOA) concentration is notably higher in winter, likely a result of more wood burning for home heating in colder months. Primary $PM_1$ accounts for about half of the total concentration in winter versus a quarter in the summer.

Comparing the result of our 2016-2017 campaign with the 2002 Pittsburgh Air Quality Study (PAQS),[32,33] the summer $PM_1$ concentration in Pittsburgh has reduced by 5.3 μg $m^{-3}$ (Figure S5b). The reduction is primarily driven by inorganic components, which fell from 9.8 to 2.8 μg $m^{-3}$. Organic aerosol concentrations increased from 4.4 to 6.2 μg $m^{-3}$.

### 3.2. Spatial patterns of $PM_1$ components

The spatial variation in primary carbonaceous PM drives the overall $PM_1$ spatial variability. The measured concentration of local BC, HOA and COA are spatially joined to 200-m grid cells in the sampling domain and are illustrated in the maps in Figure 2. The spatial variability of these factors, as well as the sum of these three, is clearly evident. In Section S.5 and Figure S5c in the supplementary information, we show that the spatial variability of local BC, HOA and COA far outweighs that of secondary components (inorganics and OOAs) and BBOA. This variability is driven by emissions from local sources; these emissions produce both intense plumes and

neighborhood-level enhancements in $PM_1$ concentrations.[25,34] In this section, we use mapping and land-use classification to investigate the details of intra-city variability of $PM_1$ concentration and sources.

### 3.2.1. Mapping of primary carbonaceous $PM_1$ components

Source-specific maps provide a reference for regulators to locate the hotspots of emission sources and can also enable epidemiologists to evaluate the health risks of PM emissions from specific sources. Emissions from different sources may vary in their risk levels,[35,36] but there is no consensus yet about what sources are more harmful. Thus, concentration maps can be useful in the advancement of exposure analysis.

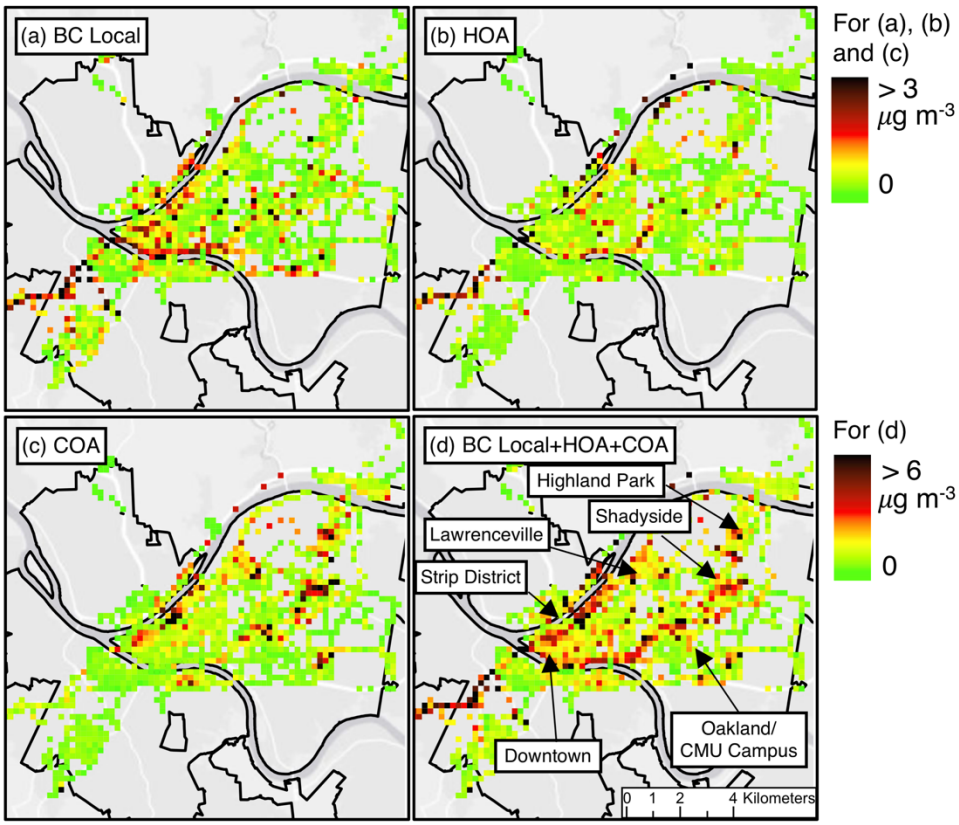


**Figure 2.** The average concentration of (a) local BC (b) HOA (c) COA and (d) total localized primary $PM_1$ in each 200m grid cell in the sampling domain. Panel (d) uses a different color scale from the rest. (Basemap attribution, Sources: Esri, DeLorme, HERE, MapmyIndia)

In Figure 2, there are important differences in the spatial patterns of local BC, HOA, and COA. For both local BC and HOA, the hotspots are located along the major truck routes. Near these truck

routes, there are sharp gradients of local BC and HOA concentrations visible on the maps. This suggests that traffic emissions can lead to high near-road concentrations, but the impacts do not reach very far beyond the scale of a single 200-meter grid cell.[37,38] Local BC concentrations are generally higher than corresponding HOA concentrations. For example, in Downtown Pittsburgh, the BC concentrations are often > 2 μg $m^{-3}$, but the HOA concentrations are ~0.5 μg $m^{-3}$, and only slightly elevated above background. This may be a result of the fleet make-up (e.g., from transit bus operations) and operating condition (e.g., stop-and-go driving) in the downtown area, or may simply reflect that emissions of organic aerosol from both gasoline and diesel vehicles have fallen rapidly in recent years.[39]

Hotspots of COA appear as clusters on the map, and spatial gradients are clearly visible at the boundary of several communities (Figure 2c). These COA hotspots arise from the clustering of restaurants in urban environments.[40] Some COA hotspots are coincident with hotspots of HOA or BC (Downtown, Strip District, Oakland and Lawrenceville), consistent with the large number of grid cells with both high traffic and high restaurant intensity. Other COA hotspots are dominated by cooking alone (Shadyside and Highland Park). Highland Park is mostly a residential area with several restaurants at the center, and the dominance of COA on the local air quality is clearly visible. In general, COA has similar, if not higher, concentrations than HOA and covers a wider range in residential area. Thus, cooking is worthy of more attention in future analysis of urban PM and OA exposure.

#### 3.2.2. Variation of $PM_1$ concentration by land-use

In this section we use the land-use classification defined in Figure 1c to evaluate the variation of PM concentration among different land-use classes. Figure 3 summarizes the average concentration and fractional contribution from each $PM_1$ component and PMF factor for three of the four land use classes: low source, traffic, and high source (restaurant plus traffic). Data collected from summer (August and September) and winter (January and February) are presented separately to contrast the seasonal trends.

We empirically determined the precision of the AMS measurement to be 0.2 μg $m^{-3}$ for most OA factors, with the exception of LOOOA and local BC (0.3 μg $m^{-3}$, Table S3 and Section S.8). This is broadly consistent with previous AMS studies.[23] In our spatial analysis, we use this precision to determine whether concentration differences among land-use classes are meaningful. This precision is inherently different from the bootstrapping method that is commonly applied in

PMF. Bootstrapping determines the uncertainty of the PMF solution itself,[27] whereas the precision defined here is used when comparing spatial concentration differences.

Local BC, HOA and COA concentrations are higher in land use classes with source impacts. Comparing traffic with low source land-use, the mean HOA concentration increases by 0.4 μg $m^{-3}$ in the summer. The difference in winter is not meaningful (0.1 μg $m^{-3}$). Local BC increases by 0.8 μg $m^{-3}$ in the summer and 0.3 μg $m^{-3}$ in the winter. The reduced impact of traffic in the winter months may be the result of differences in activity or emission factor. Vehicle volumes and miles traveled are higher in the summer.[41] Vehicle emissions may change with season or ambient temperature, though the exact relationship is uncertain, with some studies showing higher BC emissions in colder temperatures,[42] and others the reverse.[43]

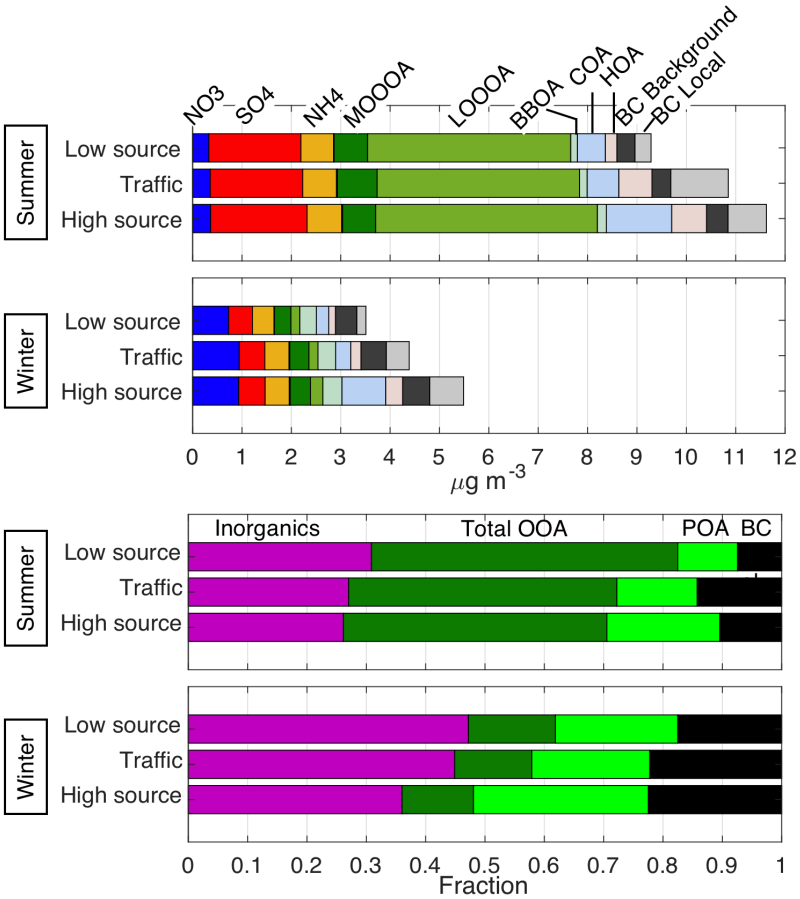


**Figure 3.** Variation of chemically-resolved $PM_1$ concentrations by land-use types in summer and winter. The top two panels show the concentrations of each specific inorganic component, OA PMF factor, and local and background BC. The bottom two panels show the fractional contribution

from broader chemical families. Total OOA = LOOOA + MOOOA. POA = primary organic aerosol = BBOA + HOA + COA.

Comparing high source (cooking added) with traffic land-use, COA concentration increases by 0.7 μg $m^{-3}$ in the summer and 0.6 μg $m^{-3}$ in the winter. The consistent spatial pattern between seasons suggests similar cooking activity patterns and emission factors in summer and winter, consistent with stationary sources of COA, primarily restaurants.[44] Overall, source-impacted areas have an additional ~1-2 μg $m^{-3}$ of primary $PM_1$ compared to low source areas.

The comparison between land-use classes discussed above uses the empirically-defined precision of OA factors and local BC to determine significant spatial differences between land-use classes. An ANOVA test also verified that the concentration differences between land use classes are statistically significant (Figure S7).

Secondary components have slight spatial variations that are season-specific. In summer, the LOOOA concentration, representative of fresh secondary organic aerosol, is enhanced in high source land-use by about 0.4 μg $m^{-3}$ compared to the other two land use types. This difference is nearly eliminated in winter (0.1 μg $m^{-3}$), largely due to reduced photochemical activity and lower total LOOOA concentrations (0.2 μg $m^{-3}$ on average). In winter, nitrate concentrations are slightly enhanced in traffic and high source land-use by 0.2 μg $m^{-3}$ compared to low source land-use, while the differences are less than 0.1 μg $m^{-3}$ in summer. The enhancement of both the LOOOA and nitrate concentration can be explained as a result of the oxidation of vehicular emissions of volatile and intermediate-volatility organic compounds and $NO_x$ in high-source areas.[45–47]

PM components typically associated with the regional background – sulfate, MOOOA, and background BC – are not spatially variable among land use classes. The differences in sulfate and MOOOA are around 0.1 μg $m^{-3}$, suggesting that these components, which form over timescales longer than ~1 day, are regionally homogeneous for this domain. Background BC has no discernable spatial pattern among the land-use classes (differences less than 0.1 μg $m^{-3}$) in both summer and winter; this is in contrast to local BC, which is elevated in high traffic areas. The spatial homogeneity of background BC verifies the background correction methods we applied, and also reflects the non-reactiveness of BC in the atmosphere. The other primary OA component, BBOA, has a seasonal difference (>0.2 μg $m^{-3}$ between summer and winter) but no spatial variation among the land-use classes in both seasons (differences less than 0.1 μg $m^{-3}$). This finding suggests

that BBOA is not an important localized source in our sampling domain and instead is likely transported from upwind locations.

Regardless of location, total OOA and inorganics are the most important contributors to $PM_1$ in both summer and winter. Primary components of $PM_1$ make up of 52% of total $PM_1$ in the worst case (high source land-use in winter) and 17% of total $PM_1$ in the best case (low source land-use in summer). In both seasons, the incremental exposure to $PM_1$ from low source to high source land-use are approximately 2 μg $m^{-3}$, and this can be largely attributed to the spatial variation of local BC, HOA, and COA concentrations.

### 3.3. Correlation between land-use covariates and $PM_1$ components

Statistical air pollutant spatial models, including land use regression (LUR), use land-use covariates to predict spatial distributions of pollution.[14,48] These covariates are generally applied to non-source specific data (e.g. PM mass) and therefore LUR attempts to attribute a fraction of measured PM mass to source categories that are related to the spatial covariates. Whether the covariates can effectively represent the concentration patterns near local sources is important to a successful LUR model.

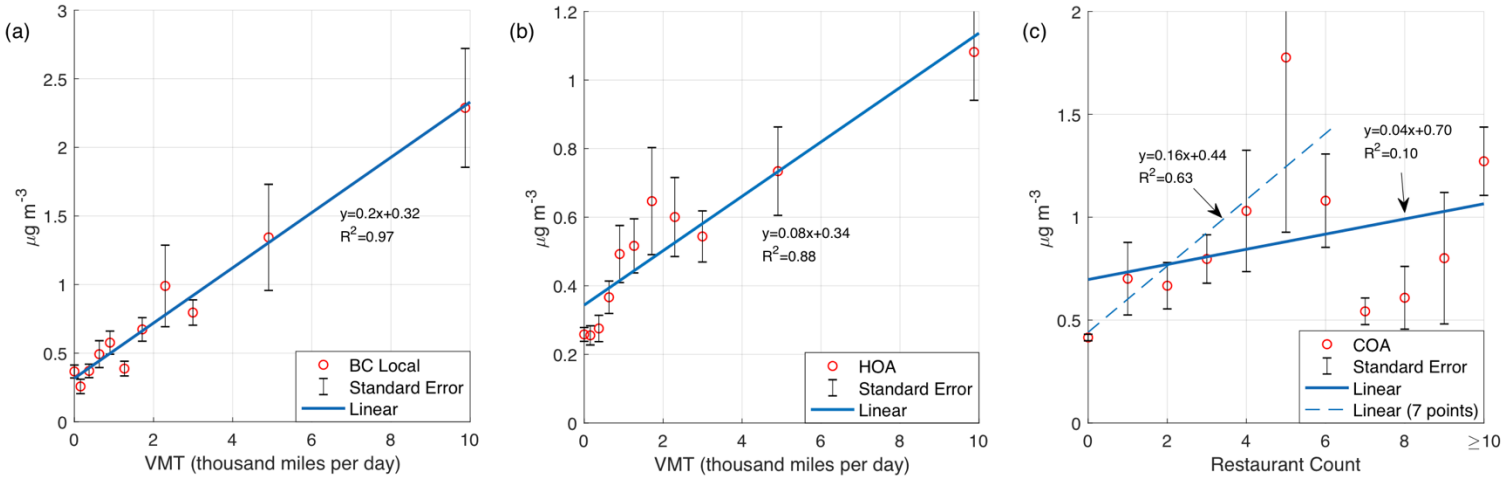


**Figure 4.** (a&b) Average concentration (red circles) and standard error (black whiskers) of local BC and HOA versus decile groups of VMT. The linear fit for the average concentrations of each group is shown as blue lines. (c) Average concentration (red circles) and standard error (black whiskers) of COA versus restaurant count. The average concentrations are calculated for groups of grid cells with the same number of restaurants inside. Cells with ten or more restaurants are

combined as one group (Table S3). Blue lines show linear fits for all (solid), as well as the first seven (dashed), data points.

We summarized the average concentration of local BC, HOA and COA for all of the 200m grid cells in our sampling domain. We also calculated values of two representative land-use covariates related to traffic and cooking emissions: annualized daily vehicle miles traveled (VMT) and restaurant counts for each grid cell. All the grid cells are binned based on decile groups of VMT and integer restaurant counts. Figure 4 shows scatter plots of mean local BC, HOA and COA concentrations of each bin against their related covariates. These figures help reveal how concentrations of primary $PM_1$ components are related to land use covariates.

The average concentrations of local BC and HOA are both linearly correlated with VMT ($R^2$=0.97 for local BC and 0.88 for HOA; Figure 4a&b). This suggests that VMT can be used as a reliable predictor of traffic-related primary PM concentration. Previous BC LURs[21,49] have leveraged this strong relationship between BC and traffic covariates.

The HOA:BC ratio is spatially variable and can be different by a factor of two depending on VMT. At lower VMT (<2000 miles per day), HOA and BC concentrations are approximately equal (HOA:BC ~ 1). For the highest traffic bin (VMT = 10,000 miles per day), the HOA:BC ratio is 0.5, suggesting higher relative emissions of BC than HOA in extremely high traffic areas.

There are two possible explanations for this phenomenon. First, the vehicle fleet composition is spatially variable. Diesel trucks constitute a larger fraction of total VMT for grid cells with VMT > 3000 miles per day (the upper three deciles) than for grid cells with VMT < 3000 miles per day (Figure S8). Diesel vehicles, especially older vehicles not equipped with advanced after treatment systems such as diesel particulate filters, have much lower HOA:BC emission ratios than gasoline vehicles.[39] Absolute BC and HOA emissions from diesel vehicles are also larger than from gasoline vehicles, so small changes in the composition of the on-road vehicle fleet can have large impacts on overall fleet emissions.[50] Thus, cells with a higher fraction of diesel truck traffic should be expected to have lower HOA:BC ratios. Second, vehicle operating conditions are also spatially variable. Grid cells with VMT>3000 miles per day are mostly highways (Figure S2), where traffic is often free-flowing at high speed. Cells with VMT <3000 miles per day are surface streets where vehicles travel at lower speed and often operate at stop-and-go conditions. The emission factors of both diesel and gasoline vehicles can vary by an order of magnitude depending on operating conditions, and there is evidence that the hot/cold start condition typical of urban

driving increases HOA emissions more than BC.[51,52] Thus, cells with stop-and-start traffic would be expected to have a higher HOA:BC ratio than cells containing highways, independent of fleet composition.

The total contribution of local traffic to $PM_1$ is the sum of local BC and HOA. The variable HOA:BC ratio in our data indicates that the total impact of traffic on $PM_1$ exposures cannot be determined from BC alone; the HOA concentration is not a linear transform of the local BC concentration. This demonstrates the value of the source-specific measurements presented here. We are able to determine the contribution of local traffic to $PM_1$ in each grid cell because of the chemical specificity of the AMS.

The relationship between COA concentration and restaurant count is complex for the entire range of data (Figure 4c). COA is linearly correlated with restaurant count for grid cells with fewer than 6 restaurants ($R^2$=0.63) but is poorly correlated ($R^2$=0.10) for the entire range. This may be an artifact of the small number of grid cells with >6 restaurants (Table S4). It may also reflect the location of restaurant exhaust hoods.[25] Areas with lower restaurant and building density may be more likely to vent cooking exhaust at street level than more congested (e.g., downtown) areas. In cities with more intense commercial activities, it may be possible to collect data in more areas with extremely high restaurant counts and improve the correlation.

We believe that restaurant count may not be a perfect indicator for cooking emissions for two main reasons. First, it excludes multiple sources of cooking emissions: household cooking, food trucks, and non-commercial outdoor grilling activities. All these activities can be significant cooking emission sources for local environments. Unfortunately, data that can reliably quantify the emissions from such sources at a high spatial resolution do not exist. Second, the emission rate of an individual restaurant may be largely dependent on the cooking style and the activity level.[53] Meat grilling can be more polluting than sushi making, and a large restaurant can have larger emissions than a smaller one with similar cooking style. These factors are not captured in the restaurant count statistics. Future analysis may benefit from more detailed information for each restaurant, such as cooking style and daily average number of guests.

COA is also correlated with traffic volume (Figure S7 and S9). For grid cells with VMT < 3000 miles per day, COA concentration increases with VMT (Figure S9). This is likely a result of many restaurants being located in high traffic areas. COA is not correlated with VMT for the highest-traffic cells (VMT > 3000 miles per day) because these cells are highways. Thus, in studies where source apportionment of PM is not available, the traffic contribution to near-road PM

concentrations may be overestimated if land use covariates associated with restaurants are not explicitly considered.

### 3.4. Source-resolved distribution of population PM exposures

$PM_1$ concentration, source impact, and the population are all spatially variable. Thus, it can be difficult to determine which emission source has the largest impact on human exposure in an urban environment. In this section, we use the spatial distribution of population to assess the spatially-resolved exposure to local primary PM from traffic (local BC+HOA) and cooking (COA) emissions. We followed methods similar to those described in Apte et al. (2015) and Brauer et al. (2016)[54,55] for use in the Global Burden of Disease study.

We ranked the average concentrations of each PM component from all the 200m grid cells and created 50 equal bins on a logarithmic scale. A sum of population from all the grid cells that fall within each bin were calculated and a population distribution is thus constructed. It is important that this process is done for each type of land-use separately. The population distribution in the sampling domain does not match the population distribution in Allegheny County – our sampling domain is biased towards high-source and high traffic areas. The bias of the sampled domain can be adjusted by the population coverage ratio ($R_{PC}$), which is described in Equation 1 and shown in Table S5.

Equation 1.

$$R_{PC} = \frac{P_S}{P_{LUT}}$$

$R_{PC}$ is the population coverage ratio for a specific type of land-use. $P_S$ is the residential population that are covered by the sampling domain in this type of land-use. $P_{LUT}$ is the actual residential population in this type of land-use in the whole county.

The population distribution for the entire Allegheny County, which includes all types of land-use, is reconstructed following Equation 2, where the population from each land-use in the $i^{th}$ bin are weighted by $R_{PC}$ and added together. A population distribution curve can be constructed for each specific PM component, and the area under each curve represents the total population in the county. This curve is then normalized for use in Figure 5 as a probability distribution.

Equation 2.

$$P_i = \sum_{N=1}^{4} \frac{P_{S(N,i)}}{R_{PC(N)}}$$

$P_i$ is the adjusted population within the $i^{th}$ bin of concentration range. $P_{S(N,i)}$ is the population within the $N^{th}$ type of land-use that are covered by the sampling domain. $R_{PC(N,i)}$ is the population coverage ratio for the $N^{th}$ type of land-use.

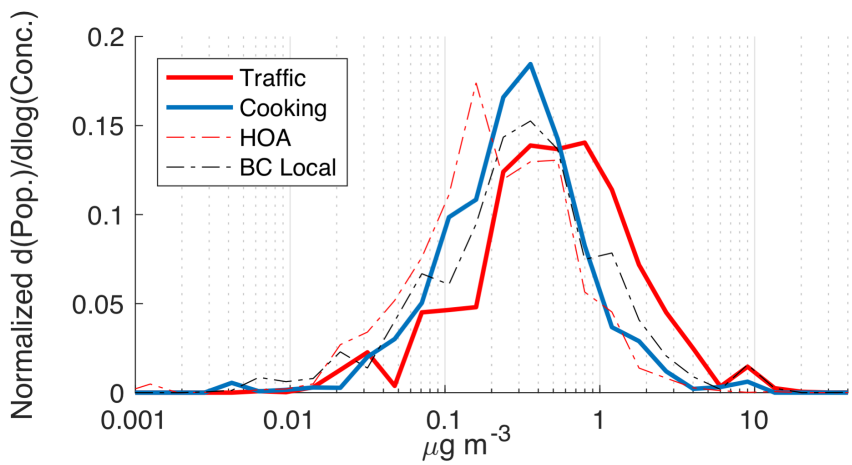


**Figure 5.** Normalized probability distribution of residential population over the measured OA and BC concentration range. The impact from traffic is the sum of the local BC and HOA concentration.

Figure 5 shows the normalized population distributions for outdoor cooking and traffic PM exposures. Each curve in Figure 5 captures the full population; the integral under every curve is unity. The four curves all follow log-normal distributions, and the medians of each curve fall between 0.1 to 1.0 μg $m^{-3}$. Primary traffic emissions are clearly more impactful than cooking on a population-weighted basis. For Allegheny county, 55%, 28% and 9% of the population are exposed to >0.5, >1 and >2 μg $m^{-3}$ of traffic-related local primary $PM_1$, respectively; the numbers for cooking-related $PM_1$ are 31%, 9% and 2%, respectively.

Cooking emissions constitute an important part of overall primary PM exposures. Curves for cooking, local BC, and HOA are similar in their medians (0.2-0.3 μg $m^{-3}$), and cooking is more important than HOA as a source of exposure to primary organic aerosol. Policies to reduce emissions from restaurant cooking, such as installation of filters on restaurant vent hoods, could

407 reduce PM exposures by ~0.3 μg $m^{-3}$ for the entire county population, with much larger reductions
408 (>1 μg $m^{-3}$) in some high-source neighborhoods with high restaurant densities.
409 Figure 5 only quantifies exposures to local primary emissions that drive a large fraction of the
410 observed intra-city spatial variability. Background BC concentrations, while spatially
411 homogeneous in our sampling domain, are at least partially the result of upwind emissions from
412 vehicular traffic. Vehicular emissions are also an important contributor to the burden of secondary
413 OA[46–48] and PM nitrate,[45] and Figure 3 shows that concentrations of the LOOOA factor, which we
414 interpret as "fresh" secondary OA, are elevated in high source areas. Thus, Figure 5 likely under
415 estimates the total PM exposure that can be assigned to vehicular emissions.
416 Probability distributions of population like those shown in Figure 5 are a useful way to examine
417 the intra-city spatial variability of outdoor $PM_1$ exposure. However, Figure 5 assumes that each
418 person's exposure is governed by the outdoor concentration at their home address. This assumption
419 may lead to exposure misclassification, because people may be exposed to emissions from indoor
420 sources[56] as well as outdoor sources, and exposures occur at places other than the home. Indoor
421 exposure is beyond the scope of this study. The proportion of indoor exposure that originates from
422 outdoor emissions can be highly variable in different environments,[57] and we lack the data to
423 reliably address this issue here. To test the sensitivity of our exposure estimates to population
424 mobility, we recalculated the population exposures using commuter-adjusted population (Figure
425 S10 and Section S.7). The overall conclusion that traffic is the major source of exposure to primary
426 PM, and that cooking is also important, is robust to the assumptions about population mobility.
427 Emissions sources in many US and European cities are dominated by traffic and cooking
428 sources. Thus, we expect to observe similar spatial patterns of PM concentration and exposure in
429 most cities, even in cases where there remain major industrial emissions sources. Preliminary
430 analysis of data collected in Oakland, CA[58] reflect the basic spatial patterns presented here: $PM_1$
431 spatial variations are dominated by carbonaceous sources, and $PM_1$ concentrations are highest in
432 source-rich environments.
433
434 **Acknowledgments**
435 This publication was developed under Assistance Agreement No. RD83587301 awarded by the
436 U.S. Environmental Protection Agency and NSF grant number AGS1543786. This publication has
437 not been reviewed by either EPA or NSF. The views expressed in this manuscript do not
438 necessarily represent those of the funding agencies. The authors would also like to thank Jiqiao

Shi, Dr. Christos Kaltsonoudis, Dr. Naomi Zimmermann, Dr. Eric Lipsky, and Rishabh Shah for help with mobile measurements and the assembly of the mobile sampling platform.

**Author Contributions**

AAP, ALR, and JSA designed research. PG, HZL, QY, and ESR performed research. PG analyzed data. PG and AAP wrote the paper with input from all authors.

## References


(1) Beelen, R.; Raaschou-Nielsen, O.; Stafoggia, M.; Andersen, Z. J.; Weinmayr, G.; Hoffmann, B.; Wolf, K.; Samoli, E.; Fischer, P.; Nieuwenhuijsen, M.; Vineis, P.; Xun, W W.; Katsouyanni, K.; Dimakopoulou, K.; Oudin, A.; Forsberg, B.; Modig, L.; Havulinna, A S.; Lanki, T.; Turunen, A.; Oftedal, B.; Nystad, W.; Nafstad, P.; De Faire, U.; Pedersen, N L.; Ostenson, C G.; Fratiglioni, L.; Penell, J.; Korek, M.; Pershagen, G.; Eriksen, K T.; Overvad, K.; Ellermann, T.; Eeftens, M.; Peeters, P H.; Meliefste, K.; Wang, M.; Bueno-de-Mesquita, B.; Sugiri, D.; Kramer, U.; Heinrich, J.; de Hoogh, K.; Key, T.; Peters, A.; Hampel, R.; Concin, H.; Nagel, G.; Ineichen, A.; Schaffner, E.; Probst-Hensch, N.; Kunzli, N.; Schindler, C.; Schikowski, T.; Adam, M.; Phuleria, H.; Vilier, A.; Clavel-Chapelon, F.; Declercq, C.; Grioni, S.; Krogh, V.; Tsai, M Y.; Ricceri, F.; Sacerdote, C.; Galassi, C.; Migliore, E.; Ranzi, A.; Cesaroni, G.; Badaloni, C.; Forastiere, F.; Tamayo, I.; Amiano, P.; Dorronsoro, M.; Katsoulis, M.; Trichopoulou, A.; Brunekreef, B.; Hoek, G. Effects of Long-Term Exposure to Air Pollution on Natural-Cause Mortality: An Analysis of 22 European Cohorts within the Multicentre ESCAPE Project. *Lancet* **2014**, *383* (9919), 785–795.

(2) Pope, C. A.; Burnett, R. T.; Thun, M. J.; Calle, E. E.; Krewski, D.; Ito, K.; Thurston, G. D. Lung Cancer, Cardiopulmonary Mortality, and Long-Term Exposure to Fine Particulate Air Pollution. *JAMA-Journal Am. Med. Assoc.* **2002**, *287* (9), 1132–1141.

(3) Eeftens, M.; Tsai, M. Y.; Ampe, C.; Anwander, B.; Beelen, R.; Bellander, T.; Cesaroni, G.; Cirach, M.; Cyrys, J.; de Hoogh, K.; De Nazelle, A.; de Vocht, F.; Declercq, C.; Dedele, A.; Eriksen, K.; Galassi, C.; Grazuleviciene, R.; Grivas, G.; Heinrich, J.; Hoffmann, B.; Iakovides, M.; Ineichen, A.; Katsouyanni, K.; Korek, M.; Kramer, U.; Kuhlbusch, T.; Lanki, T.; Madsen, C.; Meliefste, K.; Molter, A.; Mosler, G.; Nieuwenhuijsen, M.; Oldenwening, M.; Pennanen, A.; Probst-Hensch, N.; Quass, U.; Raaschou-Nielsen, O.; Ranzi, A.; Stephanou, E.; Sugiri, D.; Udvardy, O.; Vaskoevi, E.; Weinmayr, G.; Brunekreef, B.; Hoek, G. Spatial Variation of PM2.5, PM10, PM2.5 Absorbance and PMcoarse Concentrations between and within 20 European Study Areas and the Relationship with NO2 - Results of the ESCAPE Project. *Atmos. Environ.* **2012**, *62*, 303–317.

(4) Bayer-Oglesby, L.; Schindler, C.; Hazenkamp-von Arx, M. E.; Braun-Fahrlander, C.; Keidel, D.; Rapp, R.; Kunzli, N.; Braendli, O.; Burdet, L.; Liu, L. J. S.; Leuenberger, P.; Ackermann-Liebrich, U.; Team, Sapaldia. Living Near Main Streets and Respiratory Symptoms in Adults - The Swiss Cohort Study on Air Pollution and Lung Diseases in Adults. *Am. J. Epidemiol.* **2006**, *164* (12), 1190–1198.

(5) Li, H. Z.; Dallmann, T. R.; Li, X.; Gu, P.; Presto, A. A. Urban Organic Aerosol Exposure: Spatial Variations in Composition and Source Impacts. *Environ. Sci. Technol.* **2018**, *52* (2), 415–426.

(6) Krall, J. R.; Anderson, G. B.; Dominici, F.; Bell, M. L.; Peng, R. D. Short-Term Exposure to Particulate Matter Constituents and Mortality in a National Study of US Urban Communities. *Environ. Health Perspect.* **2013**, *121* (10), 1148–1153.

(7) Lanz, V. A.; Alfarra, M. R.; Baltensperger, U.; Buchmann, B.; Hueglin, C.; Prevot, A. S. H. Source Apportionment of Submicron Organic Aerosols at an Urban Site by Factor Analytical Modelling of Aerosol Mass Spectra. *Atmos. Chem. Phys.* **2007**, *7* (6), 1503–1522.

(8) Allan, J. D.; Williams, P. I.; Morgan, W. T.; Martin, C. L.; Flynn, M. J.; Lee, J.; Nemitz, E.; Phillips, G. J.; Gallagher, M. W.; Coe, H. Contributions from Transport, Solid Fuel Burning and Cooking to Primary Organic Aerosols in Two UK Cities. *Atmos. Chem.*

*Phys.* **2010**, *10* (2), 647–668.

(9) Karner, A. A.; Eisinger, D. S.; Niemeier, D. A. Near-Roadway Air Quality: Synthesizing the Findings from Real-World Data. *Environ. Sci. Technol.* **2010**, *44* (14), 5334–5344.

(10) Massoli, P.; Fortner, E. C.; Canagaratna, M. R.; Williams, L. R.; Zhang, Q.; Sun, Y.; Schwab, J. J.; Trimborn, A.; Onasch, T. B.; Demerjian, K. L.; Kolb, C E.; Worsnop, D R.; Jayne, J T. Pollution Gradients and Chemical Characterization of Particulate Matter from Vehicular Traffic Near Major Roadways: Results from the 2009 Queens College Air Quality Study in NYC. *Aerosol Sci. Technol.* **2012**, *46* (11), 1201–1218.

(11) Baccarelli, A.; Martinelli, I.; Pegoraro, V.; Melly, S.; Grillo, P.; Zanobetti, A.; Hou, L. F.; Bertazzi, P. A.; Mannucci, P. M.; Schwartz, J. Living Near Major Traffic Roads and Risk of Deep Vein Thrombosis. *Circulation* **2009**, *119* (24), 3118–3124.

(12) Brauer, M.; Lencar, C.; Tamburic, L.; Koehoorn, M.; Demers, P.; Karr, C. A Cohort Study of Traffic-Related Air Pollution Impacts on Birth Outcomes. *Environ. Health Perspect.* **2008**, *116* (5), 680–686.

(13) Bond, T. C.; Doherty, S. J.; Fahey, D. W.; Forster, P. M.; Berntsen, T.; DeAngelo, B. J.; Flanner, M. G.; Ghan, S.; Karcher, B.; Koch, D.; Kinne, S.; Kondo, Y.; Quinn, P K.; Sarofim, M C.; Schultz, M G.; Schulz, M.; Venkataraman, C.; Zhang, H.; Zhang, S.; Bellouin, N.; Guttikunda, S K.; Hopke, P K.; Jacobson, M Z.; Kaiser, J W.; Klimont, Z.; Lohmann, U.; Schwarz, J P.; Shindell, D.; Storelvmo, T.; Warren, S G.; Zender, C S. Bounding the Role of Black Carbon in the Climate System: A Scientific Assessment. *J. Geophys. Res.* **2013**, *118* (11), 5380–5552.

(14) Jedynska, A.; Hoek, G.; Wang, M.; Eeftens, M.; Cyrys, J.; Keuken, M.; Ampe, C.; Beelen, R.; Cesaroni, G.; Forastiere, F.; Cirach, M.; de Hoogh, K.; De Nazelle, A.; Nystad, W.; Declercq, C.; Eriksen, K T.; Dimakopoulou, K.; Lanki, T.; Meliefste, K.; Nieuwenhuijsen, M J.; Yli-Tuomi, T.; Raaschou-Nielsen, O.; Brunekreef, B.; Kooter, I M. Development of Land Use Regression Models for Elemental, Organic Carbon, PAH, and Hopanes/Steranes in 10 ESCAPE/TRANSPHORM European Study Areas. *Environ. Sci. Technol.* **2014**, *48* (24), 14435–14444.

(15) Robinson, A. L.; Subramanian, R.; Donahue, N. M.; Bernardo-Bricker, A.; Rogge, W. F. Source Apportionment of Molecular Markers and Organic Aerosol. 2. Biomass Smoke. *Environ. Sci. Technol.* **2006**, *40* (24), 7811–7819.

(16) Paatero, P.; Tapper, U. Positive Matrix Factorization - A Nonnegative Factor Model with Optimal Utilization of Error-Estimates of Data Values. *Environmetrics* **1994**, *5* (2), 111–126.

(17) Mohr, C.; DeCarlo, P. F.; Heringa, M. F.; Chirico, R.; Richter, R.; Crippa, M.; Querol, X.; Baltensperger, U.; Prevot, A. S. H. Spatial Variation of Aerosol Chemical Composition and Organic Components Identified by Positive Matrix Factorization in the Barcelona Region. *Environ. Sci. Technol.* **2015**, *49* (17), 10421-10430.

(18) Elser, M.; Bozzetti, C.; El-Haddad, I.; Maasikmets, M.; Teinemaa, E.; Richter, R.; Wolf, R.; Slowik, J. G.; Baltensperger, U.; Prevot, A. S. H. Urban Increments of Gaseous and Aerosol Pollutants and Their Sources Using Mobile Aerosol Mass Spectrometry Measurements. *Atmos. Chem. Phys.* **2016**, *16* (11), 7117–7134.

(19) Florou, K.; Papanastasiou, D. K.; Pikridas, M.; Kaltsonoudis, C.; Louvaris, E.; Gkatzelis, G. I.; Patoulias, D.; Mihalopoulos, N.; Pandis, S. N. The Contribution of Wood Burning and Other Pollution Sources to Wintertime Organic Aerosol Levels in Two Greek Cities. *Atmos. Chem. Phys.* **2017**, *17* (4), 3145–3163.

(20) Riley, E. A.; Banks, L.; Fintzi, J.; Gould, T. R.; Hartin, K.; Schaal, L.; Davey, M.; Sheppard, L.; Larson, T.; Yost, M. G.; Simpson, C D. Multi-Pollutant Mobile Platform

Measurements of Air Pollutants Adjacent to a Major Roadway. *Atmos. Environ.* **2014**, *98*, 492–499.

(21) Hankey, S.; Marshall, J. D. Land Use Regression Models of On-Road Particulate Air Pollution (Particle Number, Black Carbon, $PM_{2.5}$, Particle Size) Using Mobile Monitoring. *Environ. Sci. Technol.* **2015**, *49* (15), 9194–9202.

(22) Li, H. Z.; Dallmann, T. R.; Gu, P. S.; Presto, A. A. Application of Mobile Sampling to Investigate Spatial Variation in Fine Particle Composition. *Atmos. Environ.* **2016**, *142*, 71–82.

(23) DeCarlo, P. F.; Kimmel, J. R.; Trimborn, A.; Northway, M. J.; Jayne, J. T.; Aiken, A. C.; Gonin, M.; Fuhrer, K.; Horvath, T.; Docherty, K. S.; Worsnop, D R.; Jimenez, J L. Field-Deployable, High-Resolution, Time-of-Flight Aerosol Mass Spectrometer. *Anal. Chem.* **2006**, *78* (24), 8281–8289.

(24) Tan, Y.; Lipsky, E. M.; Saleh, R.; Robinson, A. L.; Presto, A. A. Characterizing the Spatial Variation of Air Pollutants and the Contributions of High Emitting Vehicles in Pittsburgh, PA. *Environ. Sci. Technol.* **2014**, *48* (24), 14186–14194.

(25) Robinson, E. S.; Gu, P.; Ye, Q.; Li, H. Z.; Shah, R. U.; Apte, J. S.; Robinson, A. L.; Presto, A. A. Restaurant Impacts on Outdoor Air Quality: Elevated Organic Aerosol Mass from Restaurant Cooking with Neighborhood-Scale Plume Extents. *Environ. Sci. Technol.* **2018**, acs.est.8b02654.

(26) Sueper, D. and Collaborators. ToF-AMS data analysis software webpage http://cires1.colorado.edu/jimenez-group/wiki/index.php/ToF-AMS_Analysis_Software.

(27) Ulbrich, I. M.; Canagaratna, M. R.; Zhang, Q.; Worsnop, D. R.; Jimenez, J. L. Interpretation of Organic Components from Positive Matrix Factorization of Aerosol Mass Spectrometric Data. *Atmos. Chem. Phys.* **2009**, *9* (9), 2891–2918.

(28) Xu, W.; Lambe, A.; Silva, P.; Hu, W.; Onasch, T.; Williams, L.; Croteau, P.; Zhang, X.; Renbaum-Wolff, L.; Fortner, E.; Jimenez, J. L.; Jayne, J. T.; Worsnop, D R..; Canagaratna, M. Laboratory Evaluation of Species-Dependent Relative Ionization Efficiencies in the Aerodyne Aerosol Mass Spectrometer. *Aerosol Sci. Technol.* **2018**, *52* (6), 626–641.

(29) Reyes-Villegas, E.; Bannan, T.; Le Breton, M.; Mehra, A.; Priestley, M.; Percival, C.; Coe, H.; Allan, J. D. Online Chemical Characterization of Food-Cooking Organic Aerosols: Implications for Source Apportionment. *Environ. Sci. Technol.* **2018**, *52* (9), 5308–5318.

(30) Robinson, A. L.; Donahue, N. M.; Rogge, W. F. Photochemical Oxidation and Changes in Molecular Composition of Organic Aerosol in the Regional Context. *J. Geophys. Res. Atmos.* **2006**, *111* (3), D03302.

(31) Zhao, B.; Wang, S.; Donahue, N. M.; Jathar, S. H.; Huang, X.; Wu, W.; Hao, J.; Robinson, A. L. Quantifying the Effect of Organic Aerosol Aging and Intermediate-Volatility Emissions on Regional-Scale Aerosol Pollution in China. *Sci. Rep.* **2016**, *6* (1), 28815.

(32) Zhang, Q.; Alfarra, M. R.; Worsnop, D. R.; Allan, J. D.; Coe, H.; Canagaratna, M. R.; Jimenez, J. L. Deconvolution and Quantification of Hydrocarbon-like and Oxygenated Organic Aerosols Based on Aerosol Mass Spectrometry. *Environ. Sci. Technol.* **2005**, *39* (13), 4938–4952.

(33) Polidori, A.; Turpin, B. J.; Lim, H. J.; Cabada, J. C.; Subramanian, R.; Pandis, S. N.; Robinson, A. L. Local and Regional Secondary Organic Aerosol: Insights from a Year of Semi-Continuous Carbon Measurements at Pittsburgh. *Aerosol Sci. Technol.* **2006**, *40* (10), 861–872.

(34) Tan, Y.; Dallmann, T. R.; Robinson, A. L.; Presto, A. A. Application of Plume Analysis to Build Land Use Regression Models from Mobile Sampling to Improve Model Transferability. *Atmos. Environ.* **2016**, *134*, 51–60.

(35) West, J. J.; Cohen, A.; Dentener, F.; Brunekreef, B.; Zhu, T.; Armstrong, B.; Bell, M. L.; Brauer, M.; Carmichael, G.; Costa, D. L.; Dockery, D W.; Kleeman, M.; Krzyzanowski, M.; Kunzli, N.; Liousse, C.; Lung, S. C. C.; Martin, R. V.; Poschl, U.; Pope, C A.; Roberts, J. M.; Russell, A. G.; Wiedinmyer, C. What We Breathe Impacts Our Health: Improving Understanding of the Link between Air Pollution and Health. *Environ. Sci. Technol.* **2016**, *50* (10), 4895–4904.

(36) Krall, J. R.; Mullholland, J. A.; Russell, A. G.; Balachandran, S.; Winquist, A.; Tolbert, P. E.; Waller, L. A.; Sarnat, S. E. Associations between Source-Specific Fine Particulate Matter and Emergency Department Visits for Respiratory Disease in Four U.S. Cities. *Environ. Heal. Perspect.* **2017**, *125*, 97–103.

(37) Gordon, M.; Staebler, R. M.; Liggio, J.; Li, S. M.; Wentzell, J.; Lu, G.; Lee, P.; Brook, J. R. Measured and Modeled Variation in Pollutant Concentration Near Roadways. *Atmos. Environ.* **2012**, *57*, 138–145.

(38) Apte, J. S.; Messier, K. P.; Gani, S.; Brauer, M.; Kirchstetter, T. W.; Lunden, M. M.; Marshall, J. D.; Portier, C. J.; Vermeulen, R. C. H.; Hamburg, S. P. High-Resolution Air Pollution Mapping with Google Street View Cars: Exploiting Big Data. *Environ. Sci. Technol.* **2017**, *51* (12), 6999–7008.

(39) May, A. A.; Nguyen, N. T.; Presto, A. A.; Gordon, T. D.; Lipsky, E. M.; Karve, M.; Gutierrez, A.; Robertson, W. H.; Zhang, M.; Brandow, C.; Chang, O.; Chen, S Y.; Cicero-Fernandez, P.; Dinkins, L.; Fuentes, M.; Huang, S M.; Ling, R.; Long, J.; Maddox, C.; Massetti, J.; McCauley, E.; Miguel, A.; Na, K.; Ong, R.; Pang, Y. B.; Rieger, P.; Sax, T.; Truong, T.; Vo, T.; Chattopadhyay, S.; Maldonado, H.; Maricq, M M.; Robinson, A. L. Gas- and Particle-Phase Primary Emissions from In-Use, On-Road Gasoline and Diesel Vehicles. *Atmos. Environ.* **2014**, *88*, 247–260.

(40) Prayag, G.; Landre, M.; Ryan, C. Restaurant Location in Hamilton, New Zealand: Clustering Patterns from 1996 to 2008. *Int. J. Contemp. Hosp. Manag.* **2012**, *24* (2–3), 430–450.

(41) PennDOT. Pennsylvania 2016 Traffic Data http://www.dot7.state.pa.us/BPR_pdf_files/MAPS/Traffic/LocalRoadProgram/allegheny.PDF.

(42) Wang, J. M.; Jeong, C.-H.; Zimmerman, N.; Healy, R. M.; Hilker, N.; Evans, G. J. Real-World Emission of Particles from Vehicles: Volatility and the Effects of Ambient Temperature. *Environ. Sci. Technol.* **2017**, *51* (7), 4081–4090.

(43) Saha, P. K.; Khlystov, A.; Snyder, M. G.; Grieshop, A. P. Characterization of Air Pollutant Concentrations, Fleet Emission Factors, and Dispersion near a North Carolina Interstate Freeway across Two Seasons. *Atmos. Environ.* **2018**, *177*, 143–153.

(44) Cabada, J. C.; Rees, S.; Takahama, S.; Khlystov, A.; Pandis, S. N.; Davidson, C. I.; Robinson, A. L. Mass Size Distributions and Size Resolved Chemical Composition of Fine Particulate Matter at the Pittsburgh Supersite. *Atmos. Environ.* **2004**, *38* (20), 3127–3141.

(45) Meng, Z.; Dabdub, D.; Seinfeld, J. H. Chemical Coupling between Atmospheric Ozone and Particulate Matter. *Science.* **1997**, *277*, 116–119.

(46) Robinson, A. L.; Donahue, N. M.; Shrivastava, M. K.; Weitkamp, E. A.; Sage, A. M.; Grieshop, A. P.; Lane, T. E.; Pierce, J. R.; Pandis, S. N. Rethinking Organic Aerosols: Semivolatile Emissions and Photochemical Aging. *Science.* **2007**, *315*, 1259–1262.

(47) Tkacik, D. S.; Lambe, A. T.; Jathar, S.; Li, X.; Presto, A. A.; Zhao, Y. L.; Blake, D.; Meinardi, S.; Jayne, J. T.; Croteau, P. L.; Robinson, A. L. Secondary Organic Aerosol Formation from In-Use Motor Vehicle Emissions Using a Potential Aerosol Mass Reactor. *Environ. Sci. Technol.* **2014**, *48* (19), 11235–11242.

(48) Eeftens, M.; Beelen, R.; de Hoogh, K.; Bellander, T.; Cesaroni, G.; Cirach, M.; Declercq, C.; Dedele, A.; Dons, E.; de Nazelle, A.; Dimakopoulou, K.; Eriksen, K.; Falq, G.; Fischer, P.; Galassi, C.; Grazuleviciene, R.; Heinrich, J.; Hoffmann, B.; Jerrett, M.; Keidel, D.; Korek, M.; Lanki, T.; Lindley, S.; Madsen, C.; Molter, A.; Nador, G.; Nieuwenhuijsen, M.; Nonnemacher, M.; Pedeli, X.; Raaschou-Nielsen, O.; Patelarou, E.; Quass, U.; Ranzi, A.; Schindler, C.; Stempfelet, M.; Stephanou, E.; Sugiri, D.; Tsai, M Y.; Yli-Tuomi, T.; Varro, M J.; Vienneau, D.; von Klot, S.; Wolf, K.; Brunekreef, B.; Hoek, G. Development of Land Use Regression Models for PM2.5, PM2.5 Absorbance, PM10 and PMcoarse in 20 European Study Areas; Results of the ESCAPE Project. *Environ. Sci. Technol.* **2012**, *46* (20), 11195–11205.

(49) Clougherty, J. E.; Kheirbek, I.; Eisl, H. M.; Ross, Z.; Pezeshki, G.; Gorczynski, J. E.; Johnson, S.; Markowitz, S.; Kass, D.; Matte, T. Intra-Urban Spatial Variability in Wintertime Street-Level Concentrations of Multiple Combustion-Related Air Pollutants: The New York City Community Air Survey (NYCCAS). *J. Expo. Sci. Environ. Epidemiol.* **2013**, *23* (3), 232–240.

(50) Grieshop, A. P.; Lipsky, E. M.; Pekney, N. J.; Takahama, S.; Robinson, A. L. Fine Particle Emission Factors from Vehicles in a Highway Tunnel: Effects of Fleet Composition and Season. *Atmos. Environ.* **2006**, *40*, S287–S298.

(51) Chen, L. F.; Liang, Z. R.; Zhang, X.; Shuai, S. J. Characterizing Particulate Matter Emissions from GDI and PFI Vehicles under Transient and Cold Start Conditions. *Fuel* **2017**, *189*, 131–140.

(52) Saliba, G.; Saleh, R.; Zhao, Y.; Presto, A. A.; Lambe, A. T.; Frodin, B.; Sardar, S.; Maldonado, H.; Maddox, C.; May, A. A.; Drozd, G. T.; Goldstein, A. H.; Russell, L. M.; Hagen, F.; Robinson, A. L. Comparison of Gasoline Direct-Injection (GDI) and Port Fuel Injection (PFI) Vehicle Emissions: Emission Certification Standards, Cold-Start, Secondary Organic Aerosol Formation Potential, and Potential Climate Impacts. *Environ. Sci. Technol.* **2017**, *51* (11), 6542–6552.

(53) Torkmahalleh, M. A.; Gorjinezhad, S.; Unluevcek, H. S.; Hopke, P. K. Review of Factors Impacting Emission/Concentration of Cooking Generated Particulate Matter. *Sci. Total Environ.* **2017**, *586*, 1046–1056.

(54) Apte, J. S.; Marshall, J. D.; Cohen, A. J.; Brauer, M. Addressing Global Mortality from Ambient $PM_{2.5}$. *Environ. Sci. Technol.* **2015**, *49* (13), 8057–8066.

(55) Brauer, M.; Freedman, G.; Frostad, J.; van Donkelaar, A.; Martin, R. V; Dentener, F.; Dingenen, R. van; Estep, K.; Amini, H.; Apte, J. S.; Balakrishnan, K.; Barregard, L.; Broday, D.; Feigin, V.; Ghosh, S.; Hopke, P. K.; Knibbs, L. D.; Kokubo, Y.; Liu, Y.; Ma, S. F.; Morawska, L.; Sangrador, J. L. T.; Shaddick, G.; Anderson, H. R.; Vos, T.; Forouzanfar, M. H.; Burnett, R. T.; Cohen, A. Ambient Air Pollution Exposure Estimation for the Global Burden of Disease 2013. *Environ. Sci. Technol.* **2016**, *50* (1), 79–88.

(56) Abdullahi, K. L.; Delgado-Saborit, J. M.; Harrison, R. M. Emissions and Indoor Concentrations of Particulate Matter and Its Specific Chemical Components from Cooking: A Review. *Atmos. Environ.* **2013**, *71* (Supplement C), 260–294.

(57) Riley, W. J.; McKone, T. E.; Lai, A. C. K.; Nazaroff, W. W. Indoor Particulate Matter of Outdoor Origin: Importance of Size-Dependent Removal Mechanisms. *Environ. Sci. Technol.* **2002**, *36* (2), 200–207.

(58) Shah, R. U.; Robinson, E. S.; Gu, P.; Robinson, A.; Apte, J. S.; Presto, A. A. High Spatial Resolution Mapping of Aerosol Composition and Sources in Oakland, California Using Mobile Aerosol Mass Spectrometry. *Atmos. Chem. Phys. Discuss.* **2018**, https://doi.org/10.5194/acp-2018-703.